



LD 11-87
IN-18-CR
330169
P-38

DEPARTMENT OF MECHANICAL ENGINEERING AND MECHANICS
COLLEGE OF ENGINEERING AND TECHNOLOGY
OLD DOMINION UNIVERSITY
NORFOLK, VIRGINIA 23529

**INTEGRATION OF MECHANISM AND CONTROL FOR
LARGE-ANGLE SLEW MANEUVERS OF FLEXIBLE STRUCTURES**

By
Meng-Sang Chew, Principal Investigator

Final Report
For the period ended August 31, 1990

Prepared for
National Aeronautics and Space Administration
Langley Research Center
Hampton, Virginia 23665

Under
Research Grant NAG-1-952
Dr. Jer-Nan Juang, Technical Monitor
SDYD-Spacecraft Dynamics Branch

(NASA-CR-187876) INTEGRATION OF MECHANISM
AND CONTROL FOR LARGE-ANGLE SLEW MANEUVERS
OF FLEXIBLE STRUCTURES Final Report, period
ended 31 Aug. 1990 (Old Dominion Univ.)
38 p

N91-18188
Unclas
0330169

CSCL 22B G3/18

February 1991

Old Dominion University Research Foundation is a not-for-profit corporation closely affiliated with Old Dominion University and serves as the University's fiscal and administrative agent for sponsored programs.

Any questions or comments concerning the material contained in this report should be addressed to:

Executive Director
Old Dominion University Research Foundation
P. O. Box 6369
Norfolk, Virginia 23508-0369

Telephone: (804) 683-4293
Fax Number: (804) 683-5290

DEPARTMENT OF MECHANICAL ENGINEERING AND MECHANICS
COLLEGE OF ENGINEERING AND TECHNOLOGY
OLD DOMINION UNIVERSITY
NORFOLK, VIRGINIA 23529

**INTEGRATION OF MECHANISM AND CONTROL FOR
LARGE-ANGLE SLEW MANEUVERS OF FLEXIBLE STRUCTURES**

By

Meng-Sang Chew, Principal Investigator

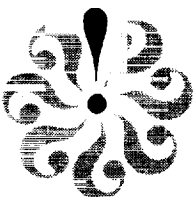
Final Report
For the period ended August 31, 1990

Prepared for
National Aeronautics and Space Administration
Langley Research Center
Hampton, Virginia 23665

Under
Research Grant NAG-1-952
Dr. Jer-Nan Juang, Technical Monitor
SDYD-Spacecraft Dynamics Branch

Submitted by the
Old Dominion University Research Foundation
P.O. Box 6369
Norfolk, Virginia 23508-0369

February 1991



INTEGRATION OF MECHANISM AND CONTROL FOR LARGE-ANGLE SLEW MANEUVERS OF FLEXIBLE STRUCTURES

M. Chew
Dept. of Mechanical Engineering and Mechanics
Old Dominion University
Norfolk, Virginia 23529-0247

ABSTRACT

A rolling contact noncircular gear system is applied to assist a desired controller in the slewing of a flexible space structure. The varying gear ratio in cooperation with the controller results in lower feedback gains at the controller, as well as considerably reduces flexural vibrations of the space structure. The noncircular gears consist of a pair of convex noncircular cylinders with specially designed profiles that are synthesized in conjunction with the optimal controller gains for minimizing the flexural vibrations of flexible structure during a slew maneuver. Convexity of the cylindrical profiles for this noncircular gear device must be ensured to maintain rolling contact between the two cylinders. Simulations of slewing control tasks for two kinds of flexible space structures, such as a planar flexible beam and the planar articulated flexible beams, will be presented.

1. INTRODUCTION

Interest in orbiting very large space structures has resulted in the need to maneuver and control flexible structures. This need is driving research into an integrated approach that incorporates mechanism synthesis and control design so that maneuvering characteristics of the large flexible space structures may be improved. Several large flexible space structures such as the Mobile Satellite, the Large Deployable Reflector, and the Freedom Space Station form the basis for much of present need for various forms of preflight testing and analysis on the ground.

In a slewing maneuver of a flexible structure under regulator feedback control, the dynamic behavior has been extensively investigated [1-4]. The choice of a regulator feedback controller is precisely due to the simplicity of such an implementation. However, the resulting flexural vibrations of the flexible structure are tunable with only the feedback gains, and are therefore not entirely satisfactory. A more direct control on the flexural vibrations on the other hand will not result in a regulator type feedback controller and will therefore be more complex in its implementation.

The objective of this article is to present an approach such that a regulator-type feedback controller may be used while incorporating some capability in varying from the regulator feedback solution. This is achieved through the incorporation of a mechanical element that transforms the feedback actuating torque so that a more desirable feedback actuation is obtained. Such a device is a noncircular gear system which will be described in the sections that follow. It may be noted that much of current controls research has been approached from the perspective, that the mechanical system is a given so that a controller is then synthesized to accomplish a given objective. However such an approach generally results in rather sophisticated feedback controllers that may not be robust. This investigation presents an approach wherein, the gains for a simple controller as well as an aspect of the mechanical system is synthesized together as an integrated design problem. In this way, a compromised is therefore afforded. A simple controller may then be used in conjunction with a slightly more complex me-

chanical system. The flexible structures that will be investigated in this article are a planar flexible beam as well as two planar articulated flexible beams equipped with the noncircular gear systems.

Several gearing devices such as gear trains and harmonic devices have been used in transmitting the actuator torques for maneuvering flexible structures [5-14]. All these transmission devices essentially exhibit constant gear ratios during a given operation. This is because circular gears always result in non-varying gear ratios between the input and output shafts of the transmission, because of the constancy of the mechanical advantage.

Based on a given desired maneuvering schedule, the gear ratio of the noncircular gears may be specified as a hyperbolic equation within the range of the slewing angle. Through the hyperbolic gear ratio, the initial input torque can be reduced, and the resulting output angular velocity will be tuned in such a way as to reduce high rates of change in a regulator type controller at the start of maneuvering. A mechanisms synthesis approach is employed to derive the design equations for the convex pitch profiles of two noncircular gears. The slewing maneuvers of two kinds of flexible space structures, i.e. a one-beam flexible structure and an articulated two-beam flexible structure, are investigated by using the designed noncircular gears to perform both positioning control tasks. The noncircular gears are installed at the junction of the motor and the flexible structure. Their regulator-type control problems are first solved using optimal control theory. Then, the resulting regulator feedback gains are applied to the system. Furthermore, an optimizer based on a nonlinear programming approach, called GRG [15-18], is employed to determine not only the pitch curves of the noncircular cylinders, but also the output feedback gains so as to will minimize the flexural vibrational amplitude. Slewing control tasks of two different flexible structures will be implemented and the flexural vibrations reduced by simultaneously taking into account the profile of the noncircular cylinders as well as output feedback controller, at the design stage. The simulation results associated with such an integrated mechanisms and control de-

sign approach are then compared to a case with just circular gears and the other with non-optimal noncircular gears.

2. EXISTING TRANSMISSION SYSTEMS

Multi-body flexible structures, generally, are maneuvered by heavy actuators in conjunction with their associated transmission systems. The transmission systems are employed to multiply and transmit torque to the adjoining ends of articulated structures. Several existing devices [5-14] have been used for transmitting the actuator torques to drive flexible structures. Some of these transmission devices are discussed below:

2.1 Gear Train

A gear train, which is made of a series of circular gears, amplifies the actuator's torque at the given constant gear ratio. The gear train can be accompanied by a roller chain or belt drive for transmitting the torque over a distance.

2.2 Harmonic Drive

This drive provides for very high gear-ratios thereby giving high drive torques but at very low backlashes.

2.3 Direct - Drive Mechanism

Special linkage mechanisms can replace the role of the complex gear train or roller chain drives in robot manipulators. Two kinds of direct-drive mechanisms have been extensively used for the rigid-body robots, such as a four-bar parallel linkage and a five-bar polygon-type linkage[11-14]. The direct-drive linkages, which are driven by two actuators located in parallel or in series, directly transmit the torques to the manipulators instead of through gear trains or roller chains, so that the actuator torques are decoupled through the direct-drive mechanisms to simplify the rather complicated coupled multi-body dynamics that mutually interacts during the control process.

One common restriction found in the prior three devices is that they can only provide non-varying gear ratios. Moreover, some performance inadequacies in using a gear train with direct drive mechanisms have been observed in their experimental setups. In the case of gear trains, backlash and friction due to the improper contact and poor surface polish of gear teeth always results in the system nonlinearity which is very difficult to compensate. Furthermore, the excessive gear inertia will complicate system dynamics. In the case of the direct drive mechanism, the entire mechanical linkage occupies precious workspace. Greater control effort is also needed to compensate for the inertia and gravity of the linkages.

In the following section, the development of a noncircular gearing device incorporating a simple control technique for manipulating slew maneuvers of two different flexible structures, will be presented.

3. DESCRIPTION OF SYSTEM

The problem of suppressing the flexural vibrations of flexible structures has inspired the development of a noncircular gear concept in conjunction with control for tuning the slewing characteristics of a flexible structure. An investigation into its applicability is the subject that will be developed in this and subsequent sections in this article. We shall begin with a brief description on non-circular gear design to serve as background. System dynamics of two different flexible structures will be derived in conjunction with their regulator-type slewing controller designs, and then the insertion of varying gear ratios associated with the proposed noncircular gears, into the previous two systems will also be presented in this section.

3.1 Mechanical Device : Noncircular Gearing Synthesis

Several noncircular gears [5-10] have been proposed in recent years and particularly in the 1950s and 1960s. Most of existing noncircular gear articles emphasized on its design for producing cyclically varying angular velocity, or for generating pre-

cise nonlinear functions from a mechanisms viewpoint. An integrated approach that incorporates the mechanism with the control has never been attempted. Moreover, the incorporation of a noncircular mechanical element permits the simplification of the control implementation and it is this objective that forms the basis of this investigation. Figure 1 shows the configuration of a pair of noncircular gears driven by a motor to rotate a flexible beam. Such a noncircular gearing device consists of:

- (1) a pair of noncircular cylinders (G_1 , G_2),
 - (2) two pairs of thin metal bands (B_1 , B_2),
 - (3) two pairs of clamps (C_1 , C_2),
- and (4) a fixed arm to hold the two cylinders at a constant distance apart.

The system features a pair of noncircular cylinders, around which two pairs of thin metal bands wrap. These two specially designed cylinders G_1 and G_2 with noncircular profiles, meshed through the use of two pairs of thin metal bands B_1 and B_2 as shown in Fig. 1. The two noncircular cylinders are wrapped in opposite directions, and are then tightly clamped by two clamps C_1 and C_2 at the two ends of the metal bands. When the profiles of the two noncircular cylinders are properly designed, pure rolling contact exists between the two cylinders. A fixed arm, which is grounded, is used to hold the two cylinders together such that the center distance always remains constant. The varying gear ratio due to the noncircular profiles produces varying output-to-input speeds. This speed variation tunes the kinematic characteristics of the flexible space structures during rapid slewing maneuvers while being controlled by a regulator-type feedback controller. Pure rolling contact, and hence low friction between the noncircular cylinders, reduces stiction nonlinearities to the system. That shear force, normally taken by the gear teeth, is taken by the bands (B_1 and B_2) in this concept.

Figure 2 demonstrates the cross section of the noncircular gears as shown in Fig. 1. Two noncircular gears O_1 and O_2 that are kept apart at a constant center distance $\overline{O_1O_2} = C$ have the instantaneous pitch radii denoted by r_1 and r_2 respectively. Assume that gears O_1 and O_2 are driving and driven gears possessing their input and

output angles, i.e. θ_1 and θ_2 . Then, their synthesis can be carried out using the concept of the varying gear ratio and has been presented in Appendix I. The pitch curves of the two noncircular cylinders are thus determined from Eqs. (I.4) and (I.5) in Appendix I. To simplify the specification of the varying gear ratio, a hyperbolic gear ratio is used and is defined as:

$$N_g(\theta_2) = \frac{\dot{\theta}_2}{\dot{\theta}_1} = \frac{c_2}{[c_1 + \theta_2]} \quad (1)$$

where c_1 and c_2 indicate two parameters which can be determined by giving two end points along the hyperbolic curve. As an example, the pitch curves of the noncircular cylinders based on the hyperbolic function given by Eq. (1) above is shown in Fig. 3(a) for the range of $0^\circ - 90^\circ$ of output rotation, and is plotted in Fig. 3(b). The synthesis process towards achieving the pitch curves for a hyperbolic gear ratio as shown in Fig. 3 will be discussed below.

During the slewing control process, the noncircular gears characterized by a hyperbolic gear ratio given by Eq. (1) will transform the output angular displacement and velocity to behave more smoothly while simultaneously suppressing the flexural vibrations. The hyperbolic gear ratio in Fig. 3(a) is obtained by specifying the parameters $c_1 = \frac{\pi}{10}$, $c_2 = \frac{\pi}{5}$ and $C = 10$. The pitch radii of two noncircular cylinders can be found from Eq. (I.4):

$$r_1 = \frac{CN_g(\theta_2)}{[1 + N_g(\theta_2)]}, \text{ and } r_2 = \frac{C}{[1 + N_g(\theta_2)]} \quad (2)$$

From Eq. (I.5), the input angle θ_1 of the driving cylinder can be computed by:

$$\theta_1 = \frac{1}{c_2} \left[c_1 \theta_2 + \frac{\theta_2^2}{2} \right] \quad (3)$$

The plots of $r_1(\theta_1)$ and $r_2(\theta_2)$ in polar coordinates would directly confirm whether the requirements of convexity are adhered to. Based on the hyperbolic gear ratio as shown in Fig. 3(a) and Eq. (1), the pitch curves of the two noncircular cylinders are given in Fig. 3(b). The convexities of the two pitch curves confirms the feasibility of the hyperbolic gear ratio for generating the profiles of these noncircular cylinders.

3.2 Actuator Dynamics

The actuator shown in Fig.1 is connected to one of the noncircular gears through an adaptor. A step-down gear box may be built-in into the actuator to proportionally magnify the varying noncircular gear ratio. The motor may be modelled by a standard armature circuit which is governed by the following differential equation:

$$I_m \ddot{\theta}_1 + \left(C_v + \frac{K_t K_b}{R_a} \right) \dot{\theta}_1 + \tau_a = \frac{K_t}{R_a} e_a \quad (4)$$

where I_m denotes the motor inertia, C_v viscous drag coefficient, K_t motor torque constant, K_b back-emf constant, R_a armature resistance, θ_1 output motor angle, e_a applied voltage for the armature, and τ_a available torque from the motor shaft. The available torque τ_a in Eq. (4) is then transformed to the driving torque τ_s through a step-down gear box ratio N_p , as well as the varying gear ratio N_g of the noncircular gears so that:

$$\tau_a = N_g N_p \tau_s \quad (5)$$

where N_p is the constant gear ratio of the step-down gear box, and τ_s is the input torque for the flexible-link structure. Since the gear ratio in Eq. (1.2) is varying, the input-output relationship between the driving and driven cylinders is governed by a nonlinear transformation which can be shown to be:

$$\begin{pmatrix} \dot{\theta}_1 \\ \ddot{\theta}_1 \end{pmatrix} = \begin{pmatrix} \frac{1}{N_g(\theta_2)} & 0 \\ -\frac{\dot{N}_g(\theta_2)}{N_g^2(\theta_2)} & \frac{1}{N_g(\theta_2)} \end{pmatrix} \begin{pmatrix} \dot{\theta}_2 \\ \ddot{\theta}_2 \end{pmatrix} \quad (6)$$

Substituting Eqs. (5) and (6) into Eq. (4), the output torque τ_s to the structure is obtained and is expressed by:

$$\tau_s = \left[\frac{K_t}{R_a N_g N_p} \right] e_a - \left[\frac{C_v + \frac{K_t K_b}{R_a}}{(N_g N_p)^2} \right] \dot{\theta}_2 + \frac{I_m}{(N_g N_p)^3} \left[N_g N_p \ddot{\theta}_2 - N_p \dot{N}_g \dot{\theta}_2 \right] \quad (7)$$

where the time rate-of-change of the gear ratio \dot{N}_g in Eq. (7) can be computed by

$$\dot{N}_g = \left[\frac{dN_g}{d\theta_2} \right] \dot{\theta}_2 \quad (8)$$

The input voltage across the actuator e_a in Eq. (7), is generated according to the active feedback controller and the varying noncircular gear ratio N_g , for driving the flexible

beam and for suppressing the flexural vibrations. System dynamics of two different flexible structures will be presented in the following section.

3.3 Dynamics of Flexible Systems Incorporating Noncircular Gearing and Actuators

The synthesis of the noncircular gears and actuator dynamics can be integrated by using Eqs. (6) and (7), where the output torque τ_s couples the actuator characteristics to the structural dynamics, so that a closed-loop control system may then be implemented. In this article, the dynamics of two different flexible space structures, i.e. a planar single beam structure (see Fig. 4) and a planar articulated two-beam structure (see Fig. 5), in conjunction with cylinder-type noncircular gear designs will be investigated. A description of introducing a closed-loop regulation control system for both flexible structures will be described in Section 3.4.

3.3.1 Planar Flexible Beam

In this subsection, a derivation of the dynamic equation of a planar flexible beam driven by a motor via a built-in gear train (see Fig. 4). The flexible beam is modeled as a cantilever beam with the fixed end located at the noncircular gears while the tip of the free end is given by $x_1 = L$. Flexural vibrations are permitted during the slewing motion of the arm. We begin with expanding the deflection of the flexible beam in modal form. Lagrange's equations [19] are then applied to derive the dynamic equations of motion. Let the state vector ξ be defined as:

$$\xi = [\theta_b, q^T]^T ; \quad q^T = [q_1, q_2, \dots, q_m] \quad (9)$$

where θ_b is the root angle of the flexible beam and q_i ($i = 1, \dots, m$) are the general coordinates corresponding to the shape functions ψ_i ($i = 1, \dots, m$) for discretizing the bending deflection of the flexible beam [20].

Assume that the damping of the flexible beam is negligible. The Lagrange's equa-

tions of motion [19] for one-beam structure is then governed by

$$\mathbf{M}\ddot{\xi} + \mathbf{K}\xi = \tau \quad (10)$$

where the inertia matrix:

$$\mathbf{M} = \begin{pmatrix} I & -\tilde{p}^T \\ -\tilde{p} & \rho L \hat{\mathbf{I}} \end{pmatrix}, \quad (11)$$

where ρ is the mass density of beam per unit length, L , the length of the beam, I , the moment of inertia of the beam, $\hat{\mathbf{I}}$, a $m \times m$ identity matrix, and $\tilde{p} = \int_0^L \rho x_1 \psi(x_1) dx_1$.

The stiffness matrix is:

$$\mathbf{K} = \text{Diag} [0, \rho L \omega^2] , \quad (12)$$

where $\omega = \text{Diag} [\omega_1, \dots, \omega_m]$ and ω_i ($i = 1, \dots, m$) are the modal frequencies of $\psi_i(x_1)$ $i = 1, \dots, m$. Furthermore, the control torque vector is:

$$\tau = [\tau_s, \mathbf{0}_{(1 \times m)}]^T \quad (13)$$

Note that τ_s in Eq. (13) is identical to τ_s derived in Eq. (7). Equation (10) governs the dynamics of a linear flexible structure.

The actuator dynamics and sensor characteristics play very important roles in the controller design. The actuator for the feedback control is a dc electric motor. Since the relationship including actuator characteristics and noncircular gearing mechanisms has been established in Eq. (7), the applied beam torque τ_s in Eq. (13) can be replaced by Eq. (7) so that:

$$\tau_s = \left[\frac{K_t}{R_a N_g N_p} \right] e_a - \left[\frac{C_v + \frac{K_t K_b}{R_a}}{(N_g N_p)^2} \right] \dot{\theta}_b + \frac{I_m}{(N_g N_p)} [N_g N_p \ddot{\theta}_b - N_p \dot{N}_g \dot{\theta}_b] \quad (14)$$

where e_a is the voltage applied into the armature. The passive damping of the entire system results from the second term of the right-hand side of Eq. (14). Instead of the conventional motor's back-emf with a constant gear ratio, the back-emf in Eq. (14) can be tuned through the varying gear ratio N_g . The angular velocity and acceleration of the motor's shaft can then be obtained by using Eq. (7).

Referring to the sensors, the rotational angle is measured by a ten-turn rotary potentiometer, whereas the angular velocity is calibrated by a tachometer. Strain

gages are used to sense the bending moments along the flexible beam. Denote c_p as a conversion factor between the beam root angle θ_b and the output voltage e_p of the potentiometer; c_t , between the beam angular velocity and the output voltage e_t ; c_s , between the strain and the strain output voltage e_0 . Suppose three strain gages are placed along the flexible beam respectively at positions x_a , x_b , and x_c . An output measurement equation can be written in the following matrix form:

$$\hat{e} = [e_p, e_0(x_a), e_0(x_b), e_0(x_c), e_t, \mathbf{0}_{(1 \times m)}]^{T} = \mathbf{C}_f [\theta_b, q^T, \dot{\theta}_b, \dot{q}^T]^{T} \quad (15)$$

where

$$\mathbf{C}_f = \text{Diag}[c_p, \mathbf{C}_\epsilon, c_t, \underbrace{0, \dots, 0}_m]$$

with

$$\mathbf{C}_\epsilon = c_s h \left[\frac{\partial^2 \psi_1}{\partial x_1 \partial x_1}(x_1), \dots, \frac{\partial^2 \psi_m}{\partial x_1 \partial x_1}(x_1) \right]$$

Each element of the matrix \mathbf{C}_ϵ is a product of the conversion factor c_s , h the half thickness of the flexible beam, and the second derivative of the corresponding mode shape to a generalized coordinate evaluated at the corresponding sensor location. The reader is directed to references [2-4] for detailed information on Eq. (15). Equation (15) therefore relates the output voltage \hat{e} to the state variables θ_b and ξ through the conversion factors of the sensors.

Substituting Eqs. (14) and (15) into Eq. (10) provides:

$$\bar{\mathbf{M}}\ddot{\xi} + \bar{\mathbf{C}}\dot{\xi} + \mathbf{K}\xi = \mathbf{B}E_a(t) \quad (16)$$

where

$$\bar{\mathbf{M}} = \mathbf{M} + \text{Diag} \left[\frac{I_m}{(N_g N_p)^2}, 0, 0, 0 \right],$$

$$\bar{\mathbf{C}} = \text{Diag} \left[\frac{1}{(N_g N_p)^2} \left(\frac{K_t K_b}{R_a} + C_v - I_m \frac{\dot{N}_g}{N_g} \right), 0, 0, 0 \right],$$

$$\mathbf{B} = \text{Diag} \left[\frac{K_t}{(R_a N_g N_p)}, 0, 0, 0 \right], \text{ and } E_a(t) = [e_a]^T$$

where e_a within the vector $E_a(t)$ is the applied voltage for the motor of the flexible beam. Equation (16) thus demonstrates a closed-loop system of a flexible one-beam

structure in conjunction with a pair of noncircular gears. Recall that the time rate-of-change of the gear ratio in damping matrix \bar{C} of Eq. (16) can be found from Eq. (8).

3.3.2 Planar Articulated Flexible Beams

The noncircular gears can also be incorporated into multibody flexible structures. An articulated two-beam structure has been designed to study the feasibility of two pairs of noncircular gears for two flexible beams. One flexible beam is articulated on the tip of the previous beam to result in an articulated flexible two-beam structure as shown in Fig. 5. Such an additional beam is also treated as a cantilevered beam. An extra actuator is required, which is concatenated axially of that for the first beam as shown in Fig. 5. The fore-beam is manipulated by this additional motor through a wire or tendon configuration. In Fig. 5, denote θ_{b1} as the root angle of the first flexible beam and θ_{b2} as the root angle of the second beam, measured relative to the previous local coordinates. The state vector similar to Eq. (9) becomes:

$$\xi = [\theta_{b1}, \theta_{b2}, q_1^T, q_2^T]^T ; \quad \begin{cases} q_1^T = [q_{11}, \dots, q_{1m_1}] \\ q_2^T = [q_{21}, \dots, q_{2m_2}] \end{cases}, \text{ and} \quad (17)$$

where q_{1i} ($i = 1, \dots, m_1$) are the general coordinates corresponding to the shape functions ψ_{1i} ($i = 1, \dots, m_1$) for discretization of the bending deflection of the first flexible beam. The quantities q_{2i} ($i = 1, \dots, m_2$) and ψ_{2i} ($i = 1, \dots, m_2$) are defined similarly for the fore-beam [19]. The input matrix for the articulated flexible beams is:

$$\tau = [\tau_{s1}, \tau_{s2}, \underbrace{0, \dots, 0}_{m_1+m_2}]^T \quad (18)$$

where τ_{s1} and τ_{s2} represent the applied torques for the two flexible beams respectively.

Application of Lagrange's equations of motion [20] to such an articulated structure leads to the following dynamic equations:

$$M\ddot{\xi} + K\xi = \tau + f(\xi, \dot{\xi}) \quad (19)$$

where $f(\xi, \dot{\xi})$ represents a nonlinear force vector in addition to the matrices as defined

in Eq. (16) and can be written as:

$$f(\xi, \dot{\xi}) = [f_1, f_2, f_3, f_4]^T ; \quad \begin{cases} f_1 = \frac{\rho L^3}{2} s\theta_{b2} \dot{\theta}_{b2}^2 - Ls\theta_{b2} (h_2^T \dot{q}_2) \dot{\theta}_{b2} , \\ f_2 = -s\theta_{b2} (\psi_1^T(L) \dot{q}_1) (h_2^T \dot{q}_2) + Ls\theta_{b2} (h_2^T \dot{q}_2) \dot{\theta}_{b1} , \\ f_3 = -\frac{\rho L^2}{2} \psi_1(L) s\theta_{b2} \dot{\theta}_{b2}^2 + s\theta_{b2} \psi_1(L) (h_2^T \dot{q}_2) \dot{\theta}_{b2} , \text{ and} \\ f_4 = -Ls\theta_2 h_2 \dot{\theta}_{b1} \dot{\theta}_{b2} + h_2 s\theta_{b2} (\psi_1^T(L) \dot{q}_1) \dot{\theta}_{b2} \end{cases} \quad (20)$$

where $h_2 = \int_0^L \rho \psi_2(x_2) dx_2$ and $s\theta_{b2} = \sin(\theta_{b2})$. The symmetrical inertia matrix M in Eq. (19) becomes:

$$M = \begin{pmatrix} 4I_1 & \frac{1}{2}\rho L^3 c\theta_{b2} & -\rho L^2 \psi_1^T(L) - p_1^T & -Lh_2^T c\theta_{b2} \\ \frac{1}{2}\rho L^3 c\theta_{b2} & I_2 & -\frac{1}{2}\rho L^2 \psi_1^T(L) c\theta_{b2} & -p_2^T \\ -\rho L^2 \psi_1(L) - p_1 & -\frac{1}{2}\rho L^2 \psi_1(L) c\theta_{b2} & \rho \psi_1(L) \psi_1^T(L) + \rho L \hat{I}_1 & h_2 \psi_1^T(L) c\theta_{b2} \\ -Lh_2 c\theta_{b2} & -p_2 & h_2 \psi_1(L) c\theta_{b2} & \rho L \hat{I}_2 \end{pmatrix} \quad (21)$$

where I_i ($i = 1, 2$) are the moments of inertia of beams #1 and #2, $p_1 = \int_0^L \rho x_1 \psi_1(x_1) dx_1$, $p_2 = \int_0^L \rho x_2 \psi_1(x_2) dx_2$, and $c\theta_{b2} = \cos(\theta_{b2})$. As defined in Eq. (11), \hat{I}_1 and \hat{I}_2 are $m_1 \times m_1$ and $m_2 \times m_2$ identity matrices respectively for discretizing bending deflections of beam #1 and #2. For the flexibility of two beams, the stiffness matrix is described by

$$K = \text{Diag} [0, 0, \rho L \omega_1^2, \rho L \omega_2^2] ; \quad \begin{cases} \omega_1 = \text{Diag} [\omega_{11}, \dots, \omega_{1m_1}] , \text{ and} \\ \omega_2 = \text{Diag} [\omega_{21}, \dots, \omega_{2m_2}] \end{cases} \quad (22)$$

There are two motors which produce the torques for the independent slewing motions of the two beams. The applied beam torque τ_{s1} for the first beam in Eq. (18) is identical to that in Eq. (14). An idler gear box (constant gear ratio N_{p2}) and a pair of noncircular gears (varying gear ratio N_{g2}) are set up for the torque transmission of the second beam. Therefore, the applied beam torque τ_{s2} is generated by

$$\tau_{s2} = \left[\frac{K_{12}}{R_{a2} N_{g2} N_{p2}} \right] e_{a2} - \left[\frac{C_{v2} + \frac{K_{12} K_{12}}{R_{a2}^2}}{(N_{g2} N_{p2})^2} \right] \dot{\theta}_{b2} + \frac{I_{m2}}{(N_{g2} N_{p2})^3} [N_{g2} N_{p2} \ddot{\theta}_{b2} - N_{p2} \dot{N}_{g2} \dot{\theta}_{b2}] \quad (23)$$

where the motor parameters for fore-beam (beam #2) are defined in the same way as those in Eq. (14). Equation (23) gives the relationship for the torque τ_{s2} for the second beam, slewing through the applied voltage e_{a2} . Then, the output measurement equation becomes:

$$\begin{aligned}\hat{e} &= [e_{p0}, e_{p1}, e_{p2}, e_{o1}(x_a), e_{o1}(x_b), e_{o2}(x_a), e_{o2}(x_b), e_{t1}, e_{t2}, \mathbf{0}_{(1 \times (m_1+m_2))}]^T \\ &= \text{Diag}[c_{p1}, c_{p2}, \mathbf{C}_{e1}, \mathbf{C}_{e2}, c_{t1}, c_{t2}, \underbrace{0, \dots, 0}_{m_1+m_2}] [\theta_{b1}, \theta_{b2}, q^T, \dot{\theta}_{b1}, \dot{\theta}_{b2}, \dot{q}^T]^T\end{aligned}\quad (24)$$

where

$$\mathbf{C}_{ei} = c_i h \begin{pmatrix} \frac{\partial^2 \psi_{i1}}{\partial x_1 \partial x_1}(x_1), \dots, \frac{\partial^2 \psi_{im_1}}{\partial x_1 \partial x_1}(x_1) \\ \frac{\partial^2 \psi_{i1}}{\partial x_2 \partial x_2}(x_2), \dots, \frac{\partial^2 \psi_{im_2}}{\partial x_2 \partial x_2}(x_2) \end{pmatrix}, \quad \text{for } i = 1, 2$$

The dynamic equations in Eq. (19) can thus be rewritten as:

$$\bar{\mathbf{M}}\ddot{\xi} + \bar{\mathbf{C}}\dot{\xi} + \mathbf{K}\xi = \mathbf{B}E_a(t) + f(\xi, \dot{\xi})\quad (25)$$

where

$$\begin{aligned}\bar{\mathbf{M}} &= \mathbf{M} + \text{Diag} \left[\frac{I_{m1}}{(N_{g1}N_{p1})^2}, \frac{I_{m2}}{(N_{g2}N_{p2})^2}, \underbrace{0, \dots, 0}_{m_1+m_2} \right], \\ \bar{\mathbf{C}} &= \text{Diag} \left[\frac{\left(\frac{K_{t1}K_{b1}}{R_{a1}} + C_{v1} - I_{m1} \frac{\dot{N}_{g1}}{N_{g1}} \right)}{(N_{g1}N_{p1})^2}, \frac{\left(\frac{K_{t2}K_{b2}}{R_{a2}} + C_{v2} - I_{m2} \frac{\dot{N}_{g2}}{N_{g2}} \right)}{(N_{g2}N_{p2})^2}, \underbrace{0, \dots, 0}_{m_1+m_2} \right], \\ \mathbf{B} &= \begin{pmatrix} \frac{K_{t1}}{(R_{a1}N_{g1}N_{p1})} & 0 \\ 0 & \frac{K_{t2}}{(R_{a2}N_{g2}N_{p2})} \\ \mathbf{0}_{((m_1+m_2) \times 2)} & \end{pmatrix}, \quad \text{and } E_a(t) = \begin{pmatrix} e_{a1} \\ e_{a2} \end{pmatrix}\end{aligned}$$

Such a form facilitates the incorporation of output feedback control, which will be the subject of discussion in the next subsection.

3.4 Regulator Feedback Controller For a Slewing Maneuver

Regulator feedback controller is a linear optimal control law to perform an asymptotically stable closed-loop system in which each state will be driven toward its equilibrium region under the control process. A simple conventional regulator-type controller in conjunction with a nonvarying gear ratio of transmission will be investigated in this subsection to implement the slewing maneuvers of two different flexible structures discussed earlier. To be applicable to the algorithm of the linear regulation control, the dynamics shown in Eq. (25) will be linearized by neglecting the nonlinear force vector

$f(\xi, \dot{\xi}) \approx 0$ along with approximating $\cos(\theta_2) \approx 1$. Then both the linear dynamic equations (16) and (25) along with their output measurement equations (15) and (24) will be transformed into a system of first order state equations so that:

$$\dot{\varepsilon} = \tilde{\mathbf{A}}\varepsilon + \tilde{\mathbf{B}}E_a; \quad \begin{cases} E_a = -\tilde{\mathbf{G}}\hat{e}, \text{ and} \\ \hat{e} = \mathbf{C}_f\varepsilon \end{cases} \quad (26)$$

where

$$\varepsilon = \begin{pmatrix} \xi \\ \dot{\xi} \end{pmatrix}, \quad \tilde{\mathbf{A}} = \begin{pmatrix} \mathbf{0} & \mathbf{I} \\ -\bar{\mathbf{M}}^{-1}\mathbf{K} & -\bar{\mathbf{M}}^{-1}\bar{\mathbf{C}} \end{pmatrix}, \quad \text{and} \quad \tilde{\mathbf{B}} = \begin{pmatrix} \mathbf{0} \\ \bar{\mathbf{M}}^{-1}\mathbf{B} \end{pmatrix}$$

The control input voltage vector E_a in Eq. (26) will be fed back into the closed loop system dynamics in Eqs. (15) and (25), where the output feedback gain matrix $\tilde{\mathbf{G}}$ is determined by the following control analysis. The control criteria for linear regulation problem is to minimize a quadratic performance index which can be written as:

$$J = \int_0^{\infty} [\hat{e}^T \mathbf{Q} \hat{e} + E_a^T \mathbf{R} E_a] dt \quad (27)$$

where the output measurement weighting matrix is indicated by $\mathbf{Q} \geq 0$, and the input weighting matrix $\mathbf{R} > 0$. The output feedback gains can be determined by:

$$\tilde{\mathbf{G}} = \mathbf{R}^{-1} \tilde{\mathbf{B}}^T \mathbf{P} \quad (28)$$

where the positive definite matrix \mathbf{P} satisfies the following algebraic Riccati equation:

$$\tilde{\mathbf{A}}^T \mathbf{P} + \mathbf{P} \tilde{\mathbf{A}} + \mathbf{C}_f^T \mathbf{Q} \mathbf{C}_f - 2\mathbf{P} \tilde{\mathbf{B}} \mathbf{R}^{-1} \tilde{\mathbf{B}}^T \mathbf{P} = \mathbf{0} \quad (29)$$

In general, a successful slewing implementation must entirely fulfill two dynamic aspects: system stability and smooth continuous behavior. The output feedback gain matrix $\tilde{\mathbf{G}}$ given by Eq. (28) can ensure the asymptotical stability of poles in the closed loop system $[\tilde{\mathbf{A}} - \tilde{\mathbf{B}}\tilde{\mathbf{G}}\mathbf{C}_f]$. As it was discussed in Section 3.1, the cylinder type noncircular gears are capable of varying the actuating torque to tune the slewing characteristics so that the control effort may be reduced. Hence, the incorporation of the noncircular gears and the feedback controller must be considered together from the perspective of an integrated design process. In the other words, in the slewing control of flexible structures the flexural vibrations of the beam are reduced by taking into account

the profile design of the noncircular cylinders as well as the output feedback controller gains, together at the design stage. An optimizer is employed to determine not only the pitch curves of the noncircular cylinders, but also the output feedback gains that will minimize the vibrational amplitudes. This incorporation of noncircular gears results in a controller design that is much simpler and more robust, for implementing a slew maneuver of flexible links in robot manipulators or of flexible structures in space. Such an integrated design approach will be presented in the following section.

4. INTEGRATION OF FEEDBACK CONTROLLER DESIGN WITH NONCIRCULAR GEAR DESIGN

For an integrated mechanisms and control design, the Generalized Reduced Gradient (GRG) method [15] is employed to determine the optimal designs of noncircular gear ratios together with control gains for suppressing flexural vibrations in a slew maneuver. This nonlinear programming approach will iterate a vector of design variables that will extremize a given function, subject to some equality and inequality constraints.

$$\text{Minimize : } F(\bar{x}); \quad \bar{x} = [x_1, x_2, x_3, \dots, x_N]^T \in R^N \quad (30)$$

$$\text{Subject to : } \begin{cases} \phi_k(\bar{x}) \geq 0; & k = 1, 2, 3, \dots, K \\ \Psi_\ell(\bar{x}) = 0; & \ell = 1, 2, 3, \dots, L \end{cases} \quad (31)$$

where

- \bar{x} : a column vector of design variables,
- N : total number of design variables,
- $F(\bar{x})$: design criteria or objective function,
- $\phi_k(\bar{x})$: K inequality constraint functions,
- $\Psi_\ell(\bar{x})$: L equality constraint functions.

Basically, the GRG algorithm is used to seek the optimal solution of the design variable vector \bar{x} to minimize a cost function $F(\bar{x})$ in a local domain which is bounded through the given upper and lower bounds of the design variables. First, a starting point \bar{x}^0 of design variables must be provided for GRG algorithm to search a feasible point. The reduced gradient is then evaluated by equating a projected reduced gradient formed through Eqs. (30) to (31). The L_2 norm of the projected reduced gradient

is then checked to determine if it is within some tolerance for convergence. If so, a constrained relative minimum of the cost function has been obtained. If not, a line search provides a search direction to locate a local minimum of $F(\bar{x})$. The line search is performed by initially taking a step in the direction calculated for the design variables. The design variables are adjusted by using Newton's method until the constraint functions given by Eqs. (31) are satisfied. The cost function is thus minimized according to such a reduced gradient algorithm.

The hyperbolic parameters of noncircular gear ratio along with regulator control gains, which are assigned as design variables, will be determined by the GRG algorithm to minimize the specified cost function. A quadratic cost function is developed for the minimization of modal vibrational amplitudes. The dynamics of the flexible structures may be expressed as a system of the first-order state equations. These first-order state equations thus indicate the equality constraint functions which must be satisfied in terms of dynamic response as the optimal design variables are being searched. Inequality constraint functions are specified to bound the gear ratios or the control torques. The GRG algorithm then numerically determines the design variables, which consist of the parameters of noncircular gear ratio and the control gains, so the flexural vibrations of the structures are minimized during the slew maneuver. In addition to the parameters for the noncircular gears and the control gains, the design variables of this integration problem will include the states of vibrational modes for the flexible structures. Assume that n multiple structures are connected through n noncircular gear pairs with m flexible modes specified for the vibrational motion of each structure in a slew maneuver. Then the design variable vector is written as:

$$\bar{x} = [c, \mathcal{G}, \varepsilon(k), \dot{\varepsilon}(k+1)]^T \quad (32)$$

where c is a $1 \times 2n$ vector of parameters for noncircular gears, $\mathcal{G} = [[\tilde{G}(i, j), j = 1, \dots, 2n(m+1)], i = 1, \dots, n]$ is a $1 \times 2n(m+1)$ vector of control gains, and $\varepsilon(k), \varepsilon(k+1)$ at two different times $t = k, k+1$ are $1 \times 2n$ state vectors in the first-order state equation at two sequential times. Number of design variables, i.e. $N = 8n + 2m$, is obtained by summing the number of elements in Eq. (32). Design

variables in Eq. (32) will be determined to minimize the cost function which is defined as:

$$F(x) = \sum_{i=1}^n \{ \varpi_i \times [\theta_{bi}(k) - \theta_{bik}]^2 + \varpi_{i+n} \times [\dot{\theta}_{bi}(k) - \dot{\theta}_{bik}]^2 \} + \sum_{i=1}^n \sum_{j=1}^m [\varpi_{ij} \times q_{ij}^2(k)] \quad (33)$$

where $\theta_{bi}(k)$ and $\dot{\theta}_{bi}(k)$ ($i = 1, 2, \dots, n$) are the slewing angles and angular velocities at time k ; θ_{bik} and $\dot{\theta}_{bik}$ are the desired states, and $q_{ij}(k)$ are the magnitudes of the vibrational modes at time k . The weighting factor for each slewing state is ϖ_i ($i = 1, 2, \dots, 2n$), and those for the magnitudes of the j -th vibrational mode of the i -th structure are denoted by ϖ_{ij} ($i = 1, 2, \dots, n; j = 1, 2, \dots, m$). The cost function attempts to control the slewing states, such as angle and angular velocity, at a given time k to some specified magnitude, while minimizing the amplitudes of vibrational modes of flexible structures. Two different types of constraints are needed: equality and inequality constraints. The equality constraint functions are provided by

$$\Psi_i(\bar{x}) = \varepsilon(k+1) - \tilde{\varepsilon}(k+1), \quad \text{for } i = 1, 2, \dots, 2n \quad (34)$$

The state vector $\tilde{\varepsilon}$ at time $k+1$ is governed by:

$$\begin{cases} \tilde{\varepsilon}(k+1) = \tilde{\mathbf{A}}\varepsilon(k) + \tilde{\mathbf{B}}E_a(k) + \tilde{\mathbf{f}}; \\ E_a(k) = \tilde{\mathbf{G}}\mathbf{C}_f\varepsilon(k) \end{cases}$$

where

$$\tilde{\mathbf{A}} = \begin{pmatrix} \mathbf{0} & \mathbf{I} \\ -\bar{\mathbf{M}}^{-1}\mathbf{K} & -\bar{\mathbf{M}}^{-1}\bar{\mathbf{C}} \end{pmatrix}, \quad \tilde{\mathbf{B}} = \begin{pmatrix} \mathbf{0} \\ \bar{\mathbf{M}}^{-1}\mathbf{B} \end{pmatrix}, \quad \text{and } \tilde{\mathbf{f}} = \begin{pmatrix} \mathbf{0} \\ \bar{\mathbf{M}}^{-1}\mathbf{f}(\xi, \xi) \end{pmatrix}$$

Equation (34) shows the first-order dynamic equations of multiple structures, which must be satisfied by the feasible design variables. Several inequality constraint functions $\phi_k(\bar{x})$ defined in Eq. (31) are specified to bound the range of each varying gear ratio and torque limitation of each motor. Furthermore, the design variables are bounded by the upper bound and lower bound vectors which are delicately selected and shown as follows.

$$\bar{x}_{max} = [c_{max}, \mathcal{G}_{max}, \varepsilon_{max}(k), \dot{\varepsilon}_{max}(k+1)]^T, \quad \text{and} \quad (35)$$

$$\bar{x}_{min} = [c_{min}, \mathcal{G}_{min}, \varepsilon_{min}(k), \dot{\varepsilon}_{min}(k+1)]^T \quad (36)$$

The approach described in this section can therefore bring about an integrated design of noncircular gears as well as the control gains so as to coordinate the actuating torque during the slewing maneuver for minimum flexural vibrations. In the following section, three different simulations will be implemented by using different mechanisms or control techniques for stabilizing and tuning 90°-slew tasks of two flexible structures using this integrated mechanisms and control design approach.

5. SIMULATIONS OF TWO DIFFERENT FLEXIBLE STRUCTURES

This section includes two simulations of 90°-slew maneuvers implemented for two different planar flexible beams, whose slewing characteristics will be tuned in conjunction with the noncircular gear device. The flexural vibration of a planar flexible beam is characterized by using three vibrational modes, while two vibrational modes are applied to each beam of an articulated flexible structure. The output feedback gains, which are needed to accomplish the position control task while simultaneously suppressing the flexural vibrations, will be implemented together with a pair of specially designed noncircular gears. An optimum hyperbolic curve is also obtained to generate the varying gear ratio, while the convexity of cylindrical profiles of the noncircular gears is maintained. For each flexible structure, three different cases will be considered for comparison. The first is with the 1:1 circular gears, the second with the noncircular gears associated with a given hyperbolic gear ratio as expressed in Section 3.1, and the third with the integration of mechanism and control design.

The parameters of such two dynamic systems, which will be used for simulations, are shown in Tables 1 and 4 in the Appendix. Their weighting matrices and resulting regulator-type control gain matrices derived in Section 3.4 are summarized in Tables 2 and 5 for the first two cases. Moreover, their parameters of noncircular gear ratio as shown in Eq. (3) are given in Tables 1 and 4 for the second case. The feasible starting values of design variables will be assigned as shown in Tables 1, 2, 4, and 5. Based on Eqs. (32) to (36), Tables 3 and 6 provide a summary of the integrated approach as

well as to the feasible parameter values for the noncircular gears and the control gains to begin the optimization process. We begin with the simulations for a single flexible beam under the three different cases discussed in the previous paragraph.

5.1 Simulations of a Planar Flexible Beam

Tables 1 and 2 in the Appendix A give summaries of the model parameters and control gain matrix of a planar flexible beam. Based on Eqs. (32) to (36), Table 3 displays an integrated optimal design for the 90° -slew maneuver of a flexible one-beam structure. The results of Figs. 6(d)-6(f), which have demonstrated the severe vibrations of the beam at 0.6 second, therefore, the state vector ε and time-rate state vector $\dot{\varepsilon}$ at that time are selected as the design variables, along with the two parameters c_1 and c_2 of noncircular gear ratio, and the control gain matrix $\tilde{\mathbf{G}}_{(1 \times 8)}$, whose initial values are used to implement the second case associated with the general noncircular gears. Therefore, there is a total of twenty-six design variables for this optimization problem. The cost function is developed to suppress the dynamic characteristics of the vibrational modes q_i and \dot{q}_i ($i = 1, 2, 3$), while simultaneously keeping the slewing angle θ and the angular velocity $\dot{\theta}$ at 0.18279 rad and 0.4529 rad/sec respectively. The equality constraint functions $\Psi_i(\bar{x})$ ($i = 1, 2, \dots, 8$) are provided by eight first-order state equations which must always be satisfied during optimization process. An inequality constraint function $\phi_1(\bar{x})$ is assigned to bound the gear ratio to be greater than 0.1. Two hyperbolic parameters are bounded from 0.1 to 6.0, and the sixteen states from -10.0 to 10.0. Two more inequality constraint functions $\phi_2(\bar{x})$ and $\phi_3(\bar{x})$ are specified to bound the control torque to be between 0.5 and 1.0 Nm. The upper/lower bounds of the design variables are also given in this table. Based on these initial values of the design variables, the starting value of cost function, $F(\bar{x}^0)$, equals 42.6998 while the final cost is 0.0068555 at the minimum of $F(\bar{x})$. The optimal design of noncircular gears is obtained by $c_{1opt} = 0.14$ and $c_{2opt} = 1.81692$ which produce a hyperbolic gear ratio. The final solution of control gains that minimizes the cost function $F(\bar{x})$ is:

$$\tilde{\mathbf{G}}_{opt} = [-0.8942, -25, -349.8, -1413.7, -1.4153, -7.79999, -0.799995, 1.69999] \quad (37)$$

which, in conjunction with optimally designed noncircular gears, could suppress the beam vibration to an even higher degree.

Three simulation results for such a 90° -slew maneuver are thus summarized and characterized by lines #1, #2, and #3 in Figs. 6(a)-6(f). The results with the 1:1 circular gears are indicated by a thin solid line #1, the results for the general noncircular gears by a dashed line #2, and the results for the integrated mechanisms and control design by a thick solid line #3. The flexible steel beam slews 90.0 degrees in 6.0 seconds as shown in Fig. 6(a). Apparently, the noncircular gears for optimal integrated design, slow down the beam slewing during the first 7 -degrees of rotation, thereby providing a smoother actuation to the desired final angle than that in the presence of the circular gears. In Fig. 6(b), three different results for the beam angular velocities damp out in approximately 6.0 seconds. The higher frequency modes are clearly observed in the results using circular gears while nearly absent in the other two results for noncircular gears (lines #2 and #3). That indicates the efficient suppression of structural vibration in the presences of noncircular gears, especially the ones for optimal integrated design. Both slewing angular velocity (lines #2 and #3) with noncircular gears illustrates a smoother trajectory after 0.8 seconds which implies that the beam slewing and vibrational motion have been tuned through the use of the noncircular gears. Moreover, the peak magnitude of the angular velocity is also significantly reduced by the optimal integrated design approach. The control torques begin at 1.0 Nm and vanish quite rapidly as shown in Fig. 6(c). It can therefore be implied that the control torque in the presence of noncircular gears for the optimal integrated design (line #3) damps out the flexural vibrations faster than those with circular gears (line #1) and general noncircular gears (line #2). Also, the vibrational modes (line #3) behave significantly lower as shown in Fig. 6(c). The behavior of the first three modes are demonstrated in Figs. 6(d)-6(f). These vibrational modes can be suppressed by output feedback control in the cases with circular gears and with general noncircular gears, and are further suppressed through optimal noncircular gears in conjunction with the feedback control. As it can be seen in Fig. 6(d), the noncircular gears for optimal integrated design (line #3)

suppress the first mode more than those with circular gears (line #1) or with general noncircular gears (line #2). At 0.3 second, the first mode with circular gears produces a peak amplitude of 0.1 units compared to 0.028 units with noncircular gears for the optimal integrated design. Figure 6(e) shows the three time-histories for the second mode. The peak amplitude of each mode is considerably reduced, particularly, based on the optimal integrated design approach. A similar situation happens in the behavior of the third mode as shown in Fig. 6(f). The simulation results in Figs. 6(a)-6(f) thus provide some insights into the slewing maneuvers of a planar flexible beam in the presence of mechanical devices such as noncircular gears.

5.2 Simulations of an Articulated Flexible Beam

In a similar way, the optimal design of noncircular gears for the flexible two-beam structure can be determined in the same way as that described in Table 3. Table 6 provides a statement of the optimization problem of noncircular gears and control gain matrix for the 90°-slew maneuver of the articulated two-beam structure. Four parameters of two noncircular gears, i.e. c_{11} , c_{12} , c_{21} and c_{22} , are the design variables which generate two hyperbolic gear ratios. Since the results of Figs. 7(g)-7(j), which are associated with 1:1 circular gears, have shown the severe oscillations of the two beams at the 0.64 second, the state vector ϵ and time-rate state vector $\dot{\epsilon}$ at that time are selected to provide an additional twenty-four design variables. The elements of control gain matrix $\tilde{G}_{(2 \times 12)}$ contribute twenty-four design variables. Hence, the number N of overall design variables is now fifty-two for this optimization problem. The quadratic cost function is derived to suppress vibrational modes of two flexible beams while simultaneously keeping the two slewing angles θ_1 , θ_2 at 0.18117 rad and 0.090778 rad respectively, and two angular velocities $\dot{\theta}_1$, $\dot{\theta}_2$ at 0.19956 rad/sec and 0.20797 rad/sec respectively. Twelve first-order state equations $\Psi_i(\bar{x})$ ($i = 1, 2, \dots, 12$) produce the equality constraint functions. Two inequality constraint functions $\Psi_1(\bar{x})$ and $\Psi_2(\bar{x})$ are given to make two gear ratios greater than 0.1. Four other inequality constraint functions $\Psi_i(\bar{x})$ ($i = 3, 4, 5, 6$) are specified to bound the two control

torques to be between 0.2 and 1.5 Nm. The four hyperbolic parameters are bounded by $\frac{\pi}{8} \sim \frac{6\pi}{11}$, $\frac{3\pi}{4} \sim \frac{\pi}{11}$, $\frac{\pi}{20} \sim \frac{\pi}{23}$ and $\frac{3\pi}{5} \sim \frac{12\pi}{23}$ respectively, while the 24 states are bounded by 10.0~ -10.0. The initial value of cost function, $F(\bar{x}^0)$, equals 21.772, which yields 0.0157333 at the minimum. The optimal solution to the parameters for the noncircular gears of the first beam are $c_{11opt}=0.29$ and $c_{12opt}=1.9$, and that for the noncircular gears of the second beam are: $c_{21opt}=0.134177$ and $c_{22opt}= 1.69386$. For the two motors, the optimal solution of the control gain obtained through GRG subroutine yields:

$$\bar{G}_{opt} = \begin{pmatrix} -0.694 & -0.084 & -7.6 & -132.3 & -0.288 & -26.2 & -1.533 \\ 0.1332 & -0.439 & 4.70607 & -18.799 & -17.875 & -236.191 & -0.043 \\ & & -0.355 & -1.999 & -1.899 & 0.3 & -0.399 \\ & & -0.741 & 0.01 & -0.606 & -3.4 & -0.399 \end{pmatrix} \quad (38)$$

Figures 7(a)-7(j) display three simulation results for such a 90°-slew maneuver. Two 90° slewing simulations of two flexible steel beams are shown for a period of eight seconds in Fig. 7(a) and 7(b) respectively. In Figs. 7(c) and 7(d), the three results show that the beam angular velocities damp out in approximately 8.0 seconds. The slewing angular velocity (line #3) illustrates the smoothest trajectory after 1.0 second which implies that the beam slewing and vibrational motion have been tuned through the use of the optimal integrated design. Moreover, the peak angular velocity magnitude is also significantly reduced by this integrated approach. Figures 7(e) and 7(f) show two control torques for beam #1 and beam #2 respectively. The optimal integrated design reduces the amplitudes of the first and second modes associated with beam #1 by 21% compared to the general noncircular gears (line #2) in Figs. 7(g) and 7(i). However, compared to the results associated with the circular gears in Figs. 7(g) and 7(i), the amplitudes of the first and second modes for beam #1 are considerably reduced by 64%. In Figs. 7(h) and 7(j), the reduction of the amplitudes of beam #2 for the first and second modes is about 38% when comparing the results for the general noncircular gears (line #2). The reduction is as high as 52%, when compared to the results associated with the circular gears (line #1). These simulation results therefore show the feasibility of the integrated mechanisms and control design approach for the multi-body slewing

maneuvers of space structures.

6. CONCLUSION

Severe flexural vibration is almost always the result of rapid and large slew-angle maneuvers of flexible space structures. An investigation of an integrated mechanisms and control approach has been conducted for tuning slewing characteristics of the flexible space structures such that the flexural vibrations can be considerably suppressed through the incorporation of a nonlinear mechanical element. A pair of noncircular gears are designed to generate a hyperbolic gear ratio by wrapping two specially shaped convex cylinders which are to mesh and roll while being constrained by two pairs of thin metal bands such that slipping and backlash are prevented. The design of the noncircular gear profiles is carried out for the slewing maneuvers of two kinds of planar flexible beam-like structures; a one-beam structure and a two-beam articulated structure. The slewing response is shown to be tuned well, and the flexural vibration is suppressed during the controlled slewing process. These simulation results indicate the crucial role of integrating mechanisms and control in the design procedure for slewing maneuvers of flexible structures.

The comparison of simulation results with the noncircular gears and the circular gears implies that the hyperbolic gear ratio has been useful for tuning slewing and for sufficiently suppressing the vibrational motion. Therefore, this synthesis investigation paves the way for integrating mechanisms design with control for rapid and large angle slew maneuvers of the flexible space structures. Such simulation results provide very useful insights for building an experimental setup in NASA-Langley.

ACKNOWLEDGEMENTS

The first and second authors wish to acknowledge the support of this investigation through NASA Grant No. NAG1-830 from the Spacecraft Dynamics Branch at NASA Langley Research Center.

REFERENCES

1. Juang, J.-N., Horta, L.G. and Robertshaw H.H., "A Slewing Control Experiments for Flexible Structures," *Journal of Guidance, Control and Dynamics*, Vol. 9, Sep.-Oct. 1986, pp. 599-607.
2. Huang, J.-K., Yang, L.-F. and Juang, J.-N., "Large Planar Maneuvers for Articulators Flexible Manipulators," *Proceedings of the Guidance, Navigation and Control Conference*, AIAA paper No. 88-4119, August 1988.
3. Juang, J.-N., Yang, L.-F., Huang, J.-K. and Macauley, R., "Rapid Rotational/Translational Maneuvering Experiments of a Flexible Steel Beam," *1989 American Control Conference*, Pittsburgh, Pennsylvania, June 21-23, 1989.
4. Juang, J.-N., Yang, L.-F., and Huang, J.-K., "Lyapunov-based Control Designs for Flexible-Link Manipulators," *AIAA/ASME/ASCE/AHS 30th Structures, Structural Dynamics and Materials Conference*, Mobile, Alabama, April 5-7, 1989.
5. Peyrebrune, H.E., "Application and Design of Noncircular Gears," *Transactions of the First Conference on Mechanisms*, Purdue University, 1953, pp.21-24.
6. Benford, B.F., "Customized Motions from Economical 'Almost Standard' Eccentric Gears," *Machine Design*, Sept. 26, 1968, pp. 151-154.
7. Cunningham, F.W., "Noncircular Gears," *Transactions of the Fifth Conference on Mechanism*, Purdue University, 1958, pp.96-103.
8. Bloomfield, B., "Noncircular Gears," *Gear Design and Application*, McGraw-Hill Book Co., 1967, pp.158-165.
9. Rappaport, S., "Elliptical Gears for Cyclic Speed Variations," *Gear Design and Applications*, McGraw-Hill Book Co., 1967, pp. 166-168.
10. Miano, S.V., "Twin Eccentric Gears," *Gear Design and Applications*, McGraw Hill Book Co., 1967, pp. 169-173.
11. Asada, H., and Kanade, T., "Design of Direct-Drive Mechanical Arms," *J. of Vibration, Acoustics, Stress and Reliability in Design*, July 1983, Vol. 105, pp. 312-316.
12. Asada, H., Kanada, T., and Takeyama, I., "Control of a Direct-Drive Arm," *J. of Dynamic Systems, Measurement and Control*, Sept. 1983, Vol. 105, pp. 136-142.
13. Asada, H. and Youcef-Toumi, K., "Analysis and Design of a Direct-Drive Arm With a Five-Bar-Link Parallel Drive Mechanism," *J. of Dynamic Systems, Measurement and Control*, Sept. 1984, Vol. 106, pp. 225-230.
14. Newman, W.S. and Hogan, N., "Time Optimal Control of Balanced Manipulators," *J. of Dynamic Systems, Measurement and Control*, June 1989, Vol. 111, pp. 187-193.
15. Gabriele, G.A., "Application of the Reduced Gradient Method to Optimal Engineering Design," M.S. Thesis, School of Mechanical Engineering, Purdue University, December 1975.
16. Powell, M.J.D., "An Efficient Method of Finding the Minimum of a Function of Several Variables without Calculating Derivatives," *Computer Journal*, Vol. 7, pp. 155-162.
17. Colville, A.R., "A Comparative Study of Nonlinear Programming Codes," *IBM New York Scientific Center Report No. 320-2949*, June 1968.
18. Fletcher, R. and Reeves, C.M., "Function Minimization by Conjugate Gradients," *Computer Journal*, Vol. 7, 1964, pp. 149-154.
19. Greenwood, D.T., *Principles of Dynamics*, Prentice-Hall, Inc., Englewood Cliffs, New Jersey.
20. Meirovitch, L., *Analytical Methods in Vibrations*, Third Printing, MacMillan Company, New York, N.Y., 1971.

Table 1: Model parameters of one flexible beam

a. <u>Beam motor:</u>			
$K_{t1} = 9.3 \times 10^{-3}$	Nm/Amp	$K_{b1} = 9.2 \times 10^{-3}$	Nm/Amp
$R_{a1} = 1.1$	Ohm	$I_{m1} = 2.3 \times 10^{-6}$	kgm^2
b. <u>Steel beam:</u>			
Length	$\bar{L} = 1.0$		m
Rigidity	$EI = 0.71$		Nm^2
Density	$\rho = 0.47916$		kg/m
Thickness	$h = 0.041 \times 10^{-2}$		m
c. <u>Parameters of noncircular gear ratio:</u>			
$c_1 = \frac{\pi}{10}$			
$c_2 = \frac{3\pi}{5}$			

Table 2: Weighting and feedback gain matrices of one flexible beam

a. <u>Weighting matrices:</u>	
State weighting matrix:	
$Q = Diag[80.0 \ 0.001 \ 0.001 \ 0.001 \ 100.0 \ 0.001 \ 0.001 \ 0.001];$	
Input weighting matrix:	
$R = [100.0];$	
b. <u>Output feedback gain matrix:</u>	
$\tilde{G} = [-0.8944 \ 0.0933 \ 0.0153 \ 0.0054 \ -1.1315 \ 0.2245 \ 0.0365 \ 0.0130].$	

Table 3: Optimization problem of noncircular gears and control gain for one flexible beam

Minimize:

$$F(x) = Q \times \{ \varpi \times [\theta_b(k) - 0.18279]^2 + (1 - \varpi) \times [\dot{\theta}_b(k) - 0.4529]^2 + \sum_{i=1}^3 [\varpi \times q_i^2(k)] \}$$

where the weighting numbers $Q = 10000.00$ and $\varpi = 0.55$.

Design variables:

$$\bar{x} = [c_1, c_2, \mathcal{G}_{(1 \times 8)}, \xi(k), \dot{\xi}(k+1)]^T$$

where integers $k, k+1$ indicate time sequences and

$$\varepsilon(k) = [\theta_b(k), q_1(k), q_2(k), q_3(k), \dot{\theta}_b(k), \dot{q}_1(k), \dot{q}_2(k), \dot{q}_3(k)]^T;$$

$$\varepsilon(k+1) = [\dot{\theta}_b(k+1), \dot{q}_1(k+1), \dot{q}_2(k+1), \dot{q}_3(k+1), \ddot{\theta}_b(k+1), \ddot{q}_1(k+1), \ddot{q}_2(k+1), \ddot{q}_3(k+1)]^T.$$

Subject to:

(1) Equality constraint functions:

$$\begin{cases} \Psi_i(\bar{x}) = \varepsilon(k+1) - \bar{\varepsilon}(k+1), \text{ for } i = 1, 2, 3, \dots, 8 \\ \bar{\varepsilon}(k+1) = \tilde{\mathbf{A}}\xi(k) + \tilde{\mathbf{B}}u(k), \text{ and } u(k) = \tilde{\mathbf{G}}_{(1 \times 8)}\varepsilon(k) \end{cases}$$

where the formats of $\tilde{\mathbf{A}}$ and $\tilde{\mathbf{B}}$ have been defined in Eq. (34) and matrices $\tilde{\mathbf{M}}, \mathbf{K}$, and $\tilde{\mathbf{C}}$ have been shown in Eqs. (12) and (16).

(2) Inequality constraint functions:

$$\begin{cases} \phi_1(\bar{x}) = c_2 - 0.1 \times [c_1 + \frac{10.40413\pi}{180}] \geq 0, \\ \phi_2(\bar{x}) = -u(k) + 1.0 \geq 0, \text{ and } \phi_3(\bar{x}) = u(k) - 0.5 \geq 0. \end{cases}$$

Starting point:

$$\begin{aligned} \bar{x}^0 = & [0.153083, 1.81478, -0.8944, -19.0884, -160.9831, -449.1275, -1.5449, -4.7363, 0.2093, \\ & 0.5421, 0.18159, 0.050333, -0.0004777, -0.0000778, 0.53284, -0.01669, -0.00444, \\ & 0.00049, 0.53376, -0.017172, -0.00398, 0.000986, 0.84918, -0.43872, 0.42355, 0.45771]^T \end{aligned}$$

Bounds on design variables:

(1) Upper bounds:

$$\bar{x}_{max} = [0.16, 1.82, -0.8942, -25, -349.2, -1413.1, -1.4, -7.2, -0.2, 1.7, 16 \times [10]^T];$$

(2) Lower bounds:

$$\bar{x}_{min} = [0.14, 1.8, -0.8946, -25.6, -349.8, -143.7, -2, -7.8, -0.8, 1.1, 16 \times [-10]]^T.$$

Table 4: Model parameters of an articulated flexible beam

a. <u>Beam motors:</u>					
(1)Beam #1 motor:			(2)Beam #2 motor:		
$K_{t1} = 0.0346$	Nm/Amp		$K_{t2} = 9.3 \times 10^{-3}$	Nm/Amp	
$K_{b1} = 0.0342$	$Volt\text{-}sec/rad$		$K_{b2} = 9.2 \times 10^{-3}$	$Volt\text{-}sec/rad$	
$R_{a1} = 4$	Ohm		$R_{a2} = 1.1$	Ohm	
$I_{m1} = 4.7 \times 10^{-6}$	kgm^2		$I_{m2} = 2.3 \times 10^{-6}$	kgm^2	
$N_{p1} = 1$			$N_{p2} = 1$		
b. <u>Steel beam:</u>					
Length	$\bar{L} = 1.0$	m			
Rigidity	$EI = 0.71$	Nm^2			
Density	$\rho = 0.47916$	kg/m			
Thickness	$h = 0.041 \times 10^{-2}$	m			
c. <u>Parameters of noncircular gear ratio:</u>					
(1)Beam #1 gears:			(2)Beam #2 gears:		
$c_{11} = \frac{\pi}{10}$			$c_{21} = \frac{\pi}{44}$		
$c_{12} = \frac{3\pi}{5}$			$c_{22} = \frac{3\pi}{11}$		

Table 5: Weighting and feedback gain matrices of an articulated flexible beam

a. <u>Weighting matrices:</u>					
State weighting matrix:					
$Q = Diag [250 \ 100 \ 10 \ 10 \ 10 \ 10 \ 250 \ 100 \ 10 \ 10 \ 10 \ 10] ;$					
Input weighting matrix:					
$R = [500, \ 500] ;$					
b. <u>Output feedback gain matrix:</u>					
$\tilde{G} = \begin{pmatrix} -0.7018 & -0.0547 & 0.5633 & 2.4793 & -0.2597 & 1.3766 \\ 0.0864 & -0.4439 & 0.0345 & 4.9427 & -0.2104 & -2.9872 \\ -1.1214 & -0.2117 & 0.8029 & -0.6719 & 0.3141 & 0.0668 \\ -0.0844 & -0.5758 & 0.2477 & -0.3145 & 0.2148 & 0.0165 \end{pmatrix}$					

Table 6: Optimization problem of noncircular gears and control gain for an articulated flexible beam

Minimize:

$$F(x) = Q \times \{ \varpi_1 \times [\theta_{b1}(k) - 0.18117]^2 + (1 - \varpi_1) \times [\theta_{b2}(k) - 0.090778]^2 + \varpi_2 \times [\dot{\theta}_{b1}(k) - 0.19956]^2 + (1 - \varpi_2) \times [\dot{\theta}_{b2}(k) - 0.20792]^2 + \sum_{i=1}^2 [\varpi_1 \times q_{i1}^2(k) + (1 - \varpi_1) \times q_{i2}^2(k)] \}$$

where the weighting numbers $Q = 10000.00$, $\varpi_1 = 0.55$ and $\varpi_2 = 0.5$.

Design variables:

$$\bar{x} = [c_{11}, c_{12}, c_{21}, c_{22}, \mathcal{G}_{(1 \times 24)}, \varepsilon(k), \dot{\varepsilon}(k+1)]^T$$

where integers $k, k+1$ indicate time sequences and

$$\varepsilon(k) = [\theta_{b1}(k), \theta_{b2}(k), q_{11}(k), q_{12}(k), q_{21}(k), q_{22}(k), \dot{\theta}_{b1}(k), \dot{\theta}_{b2}(k), \dot{q}_{11}(k), \dot{q}_{12}(k), \dot{q}_{21}(k), \dot{q}_{22}(k)]^T ;$$

$$\varepsilon(k+1) = [\theta_{b1}(k+1), \theta_{b2}(k+1), q_{11}(k+1), q_{12}(k+1), q_{21}(k+1), q_{22}(k+1), \dot{\theta}_{b1}(k+1), \dot{\theta}_{b2}(k+1), \dot{q}_{11}(k+1), \dot{q}_{12}(k+1), \dot{q}_{21}(k+1), \dot{q}_{22}(k+1)]^T.$$

Subject to:

(1) Equality constraint functions:

$$\begin{cases} \Psi_i(\bar{x}) = \varepsilon(k+1) - \tilde{\varepsilon}(k+1), \text{ for } i = 1, 2, 3, \dots, 12 \\ \tilde{\varepsilon}(k+1) = \tilde{A}\varepsilon(k) + \tilde{B}u(k) + \tilde{f}, \text{ and } u(k) = \tilde{G}_{(2 \times 12)}\varepsilon(k) \end{cases}$$

where the formats of \tilde{A} , \tilde{B} and \tilde{f} have been defined in Eq. (34) and matrices \tilde{M} , K , \tilde{C} , B , and f have been shown in Eqs. (22) and (25).

(2) Inequality constraint functions:

$$\begin{cases} \phi_1(\bar{x}) = c_{12} - 0.1 \times \left[c_{11} + \frac{10.38044\pi}{180} \right] \geq 0, \\ \phi_2(\bar{x}) = c_{22} - 0.1 \times \left[c_{21} + \frac{5.201172\pi}{180} \right] \geq 0, \\ \phi_3(\bar{x}) = -u_1(k) + 1.5 \geq 0, \quad \phi_4(\bar{x}) = u_1(k) - 0.2 \geq 0, \\ \phi_5(\bar{x}) = -u_2(k) + 1.5 \geq 0, \quad \phi_6(\bar{x}) = u_2(k) - 0.2 \geq 0 \end{cases}$$

Starting point:

$$\bar{x}^0 = \left[\frac{\pi}{10}, \frac{3\pi}{5}, \frac{\pi}{22}, \frac{6\pi}{11}, -0.702, 0.086, -0.055, -0.444, -7.845, 4.965, -132.538, -18.617, -0.193, -17.848, -26.478, -236.05, -1.121, -0.084, -0.212, -0.576, -1.867, 0.219, -1.798, -0.888, 0.588, -3.278, -0.221, -0.218, 0.1812, 0.09078, 0.063, -0.0012, 0.016, 0.000264, 0.2, 0.208, -0.0062, 0.0039, -0.0051, 0.0016, 0.2, 0.208, -0.0064, 0.0039, -0.0049, 0.0015, -0.088, 0.914, -0.281, -0.03, 0.3, -0.071 \right]^T.$$

Bounds on design variables:

(1) Upper bounds:

$$\bar{x}_{max} = [0.3, 1.9, 0.16, 1.73, -0.69, 0.13, -0.08, -0.44, -7.6, 5.1, -132.3, -18.4, -0.08, -17.6, -26.2, -235.8, -1.53, -0.04, -0.36, -0.74, -1.6, 0.4, -1.5, -0.6, 0.7, -3.0, -0.02, -0.01, 24 \times [10]]^T$$

(2) Lower bounds:

$$\bar{x}_{min} = [0.29, 1.86, 0.12, 1.69, -0.69, 0.13, -0.08, -0.44, -8.0, 4.7, -132.7, -18.8, -0.3, -18.0, -26.6, -236.2, -1.53, -0.04, -0.36, -0.74, -2.0, 0.01, -1.9, -1.0, 0.3, -3.4, -0.4, -0.4, 24 \times [-10]]^T.$$

APPENDIX I: NONCIRCULAR GEARING SYNTHESIS

The profiles of a pair of noncircular cylinders as shown in Fig. 1 can be developed using the following gearing synthesis. Figure 2 shows the cross section of two noncircular gears centered at O_1 and O_2 with the pitch radii r_1 and r_2 respectively. Their angular displacements are indicated by θ_1 and θ_2 , angular velocities $\dot{\theta}_1$ and $\dot{\theta}_2$, and angular acceleration $\ddot{\theta}_1$ and $\ddot{\theta}_2$ respectively. The center distance $\overline{O_1O_2}$ is denoted by C and the pressure angle by ϕ . The necessary conditions for rolling contact between two gears O_1 and O_2 as shown in Fig. 2 are:

- (1) Contact point is aligned along their center-to-center line $\overline{O_1O_2}$,
- (2) The equivalent tracking arc length must satisfy the relationship:

$$da = db \Rightarrow r_1 d\theta_1 = r_2 d\theta_2 \quad (I.1)$$

where $d\theta_1$ and $d\theta_2$ are the small angular displacements of gears O_1 and O_2 respectively. Suppose that the varying gear ratio $N_g(\theta_2)$ is defined as the ratio of the output to input angular velocities, then:

$$N_g(\theta_2) = \frac{\dot{\theta}_2}{\dot{\theta}_1} = \frac{r_1}{r_2} \quad (I.2)$$

where r_1 and r_2 are the instantaneous pitch radii of driving and driven gears respectively. The center distance C between the cylinders is a constant and must satisfy:

$$r_1 + r_2 = C \quad (I.3)$$

From this, the pitch radii r_1 and r_2 of the two noncircular cylinders can be shown to be:

$$r_1 = \frac{CN_g(\theta_2)}{[1 + N_g(\theta_2)]}, \quad r_2 = \frac{C}{[1 + N_g(\theta_2)]} \quad (I.4)$$

The input angle θ_1 of the driving cylinder O_1 can be computed by integrating Eq. (I.2) as given by:

$$\theta_1 = \int_0^{\theta_2} \left[\frac{1}{N_g(\theta_2)} \right] d\theta_2 \quad (I.5)$$

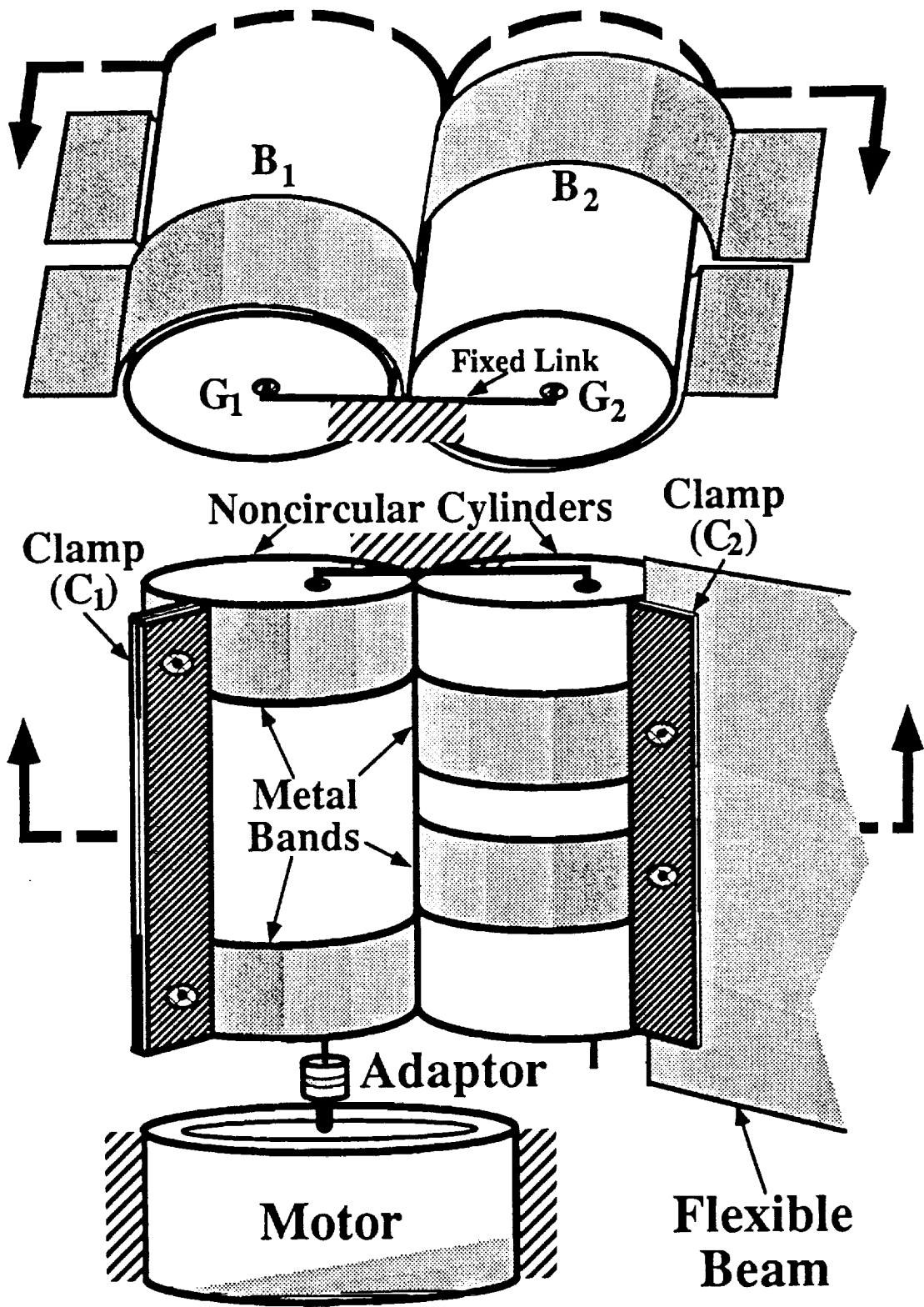


Figure 1: A pair of noncircular gears wrapped via thin bands

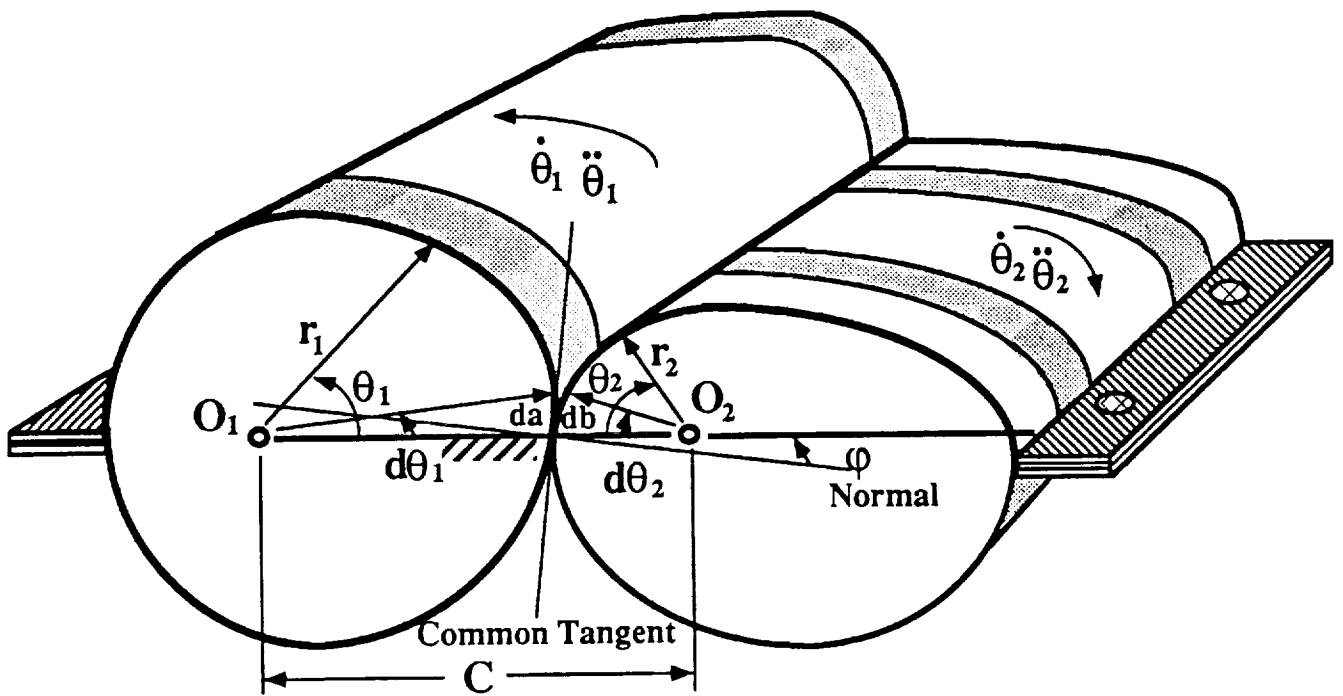


Figure 2: Configuration of noncircular gears

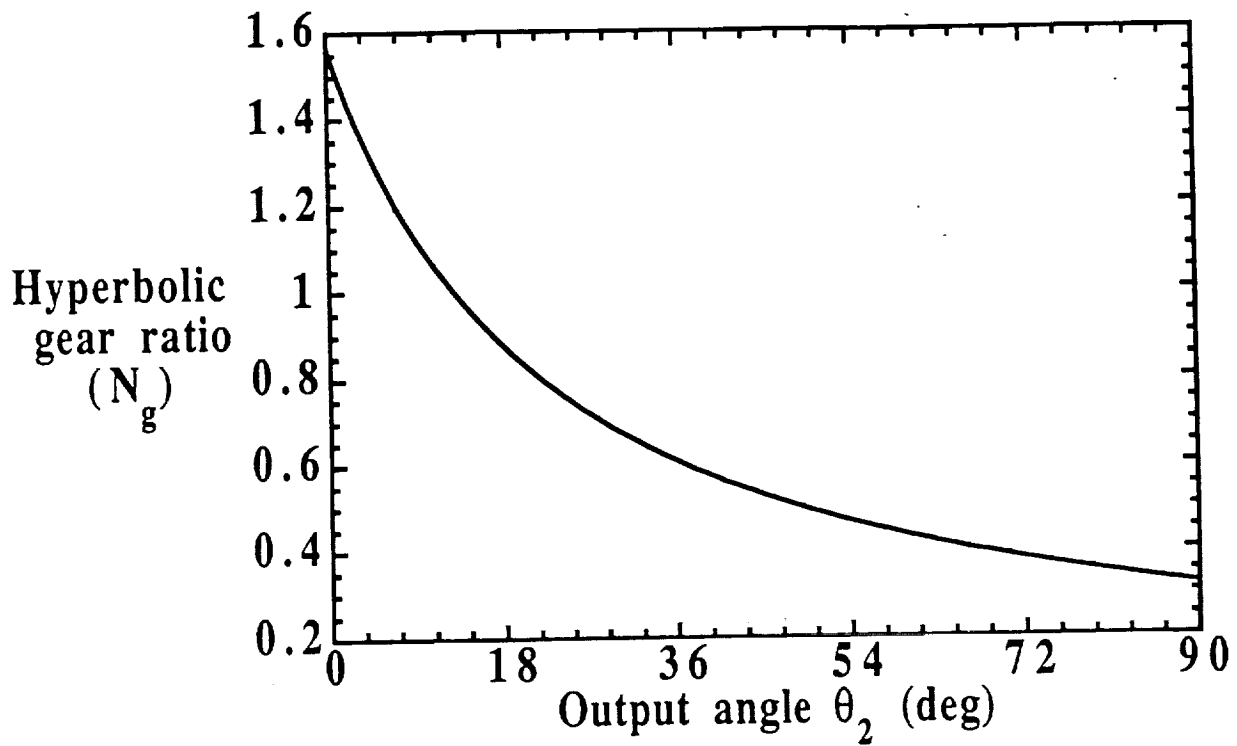


Figure 3(a): Hyperbolic gear ratio as a function of driven gear rotation angle

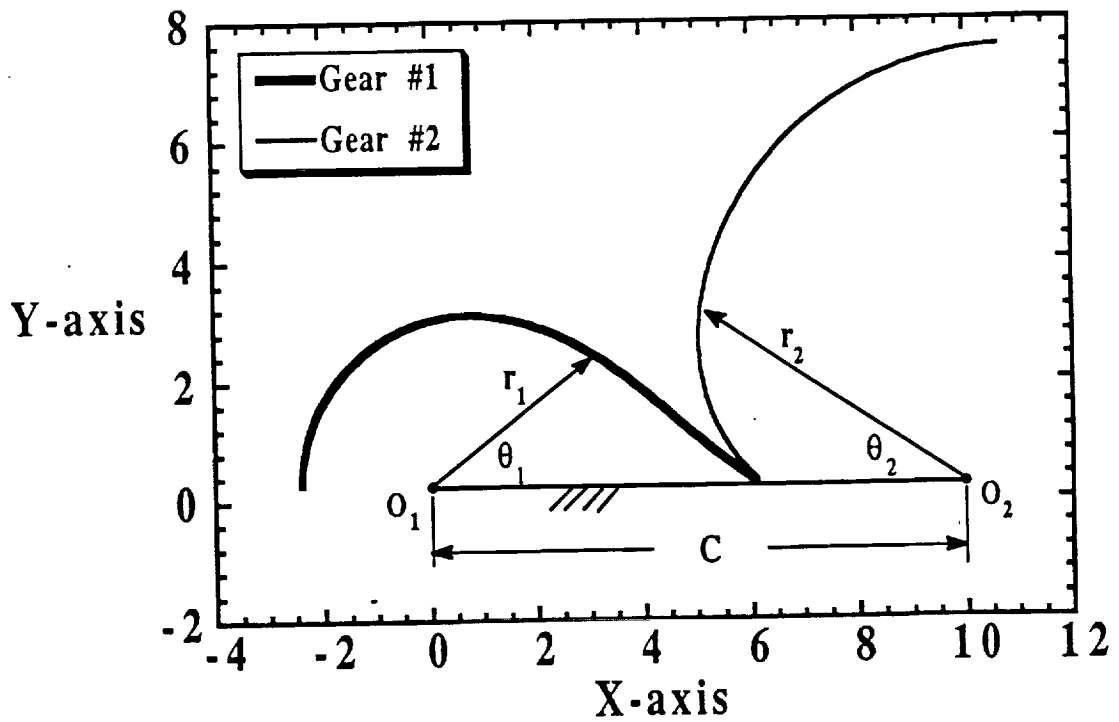


Figure 3(b): Profiles of noncircular gears with a hyperbolic gear ratio

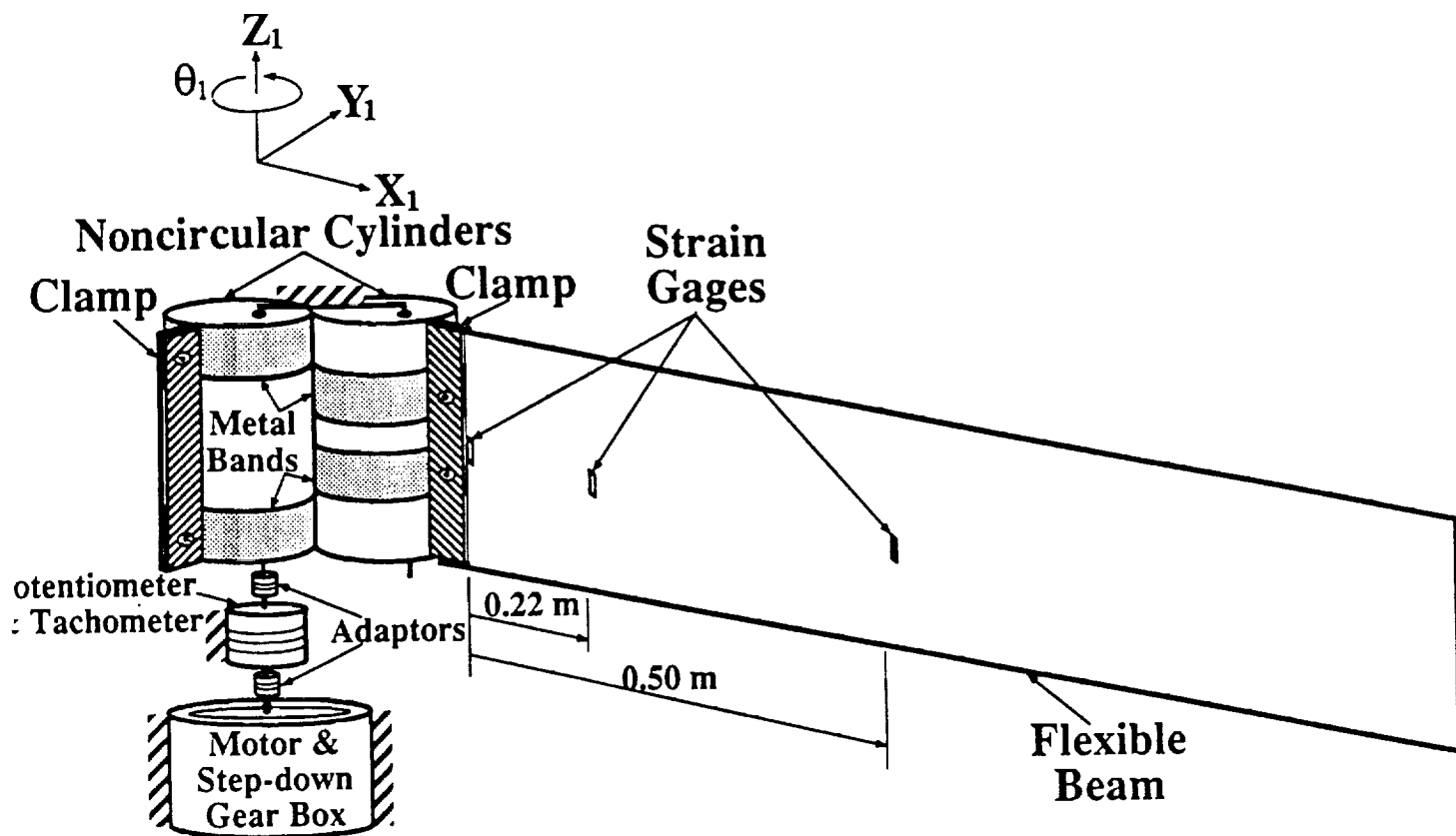


Figure 4: Configuration of a planar flexible beam

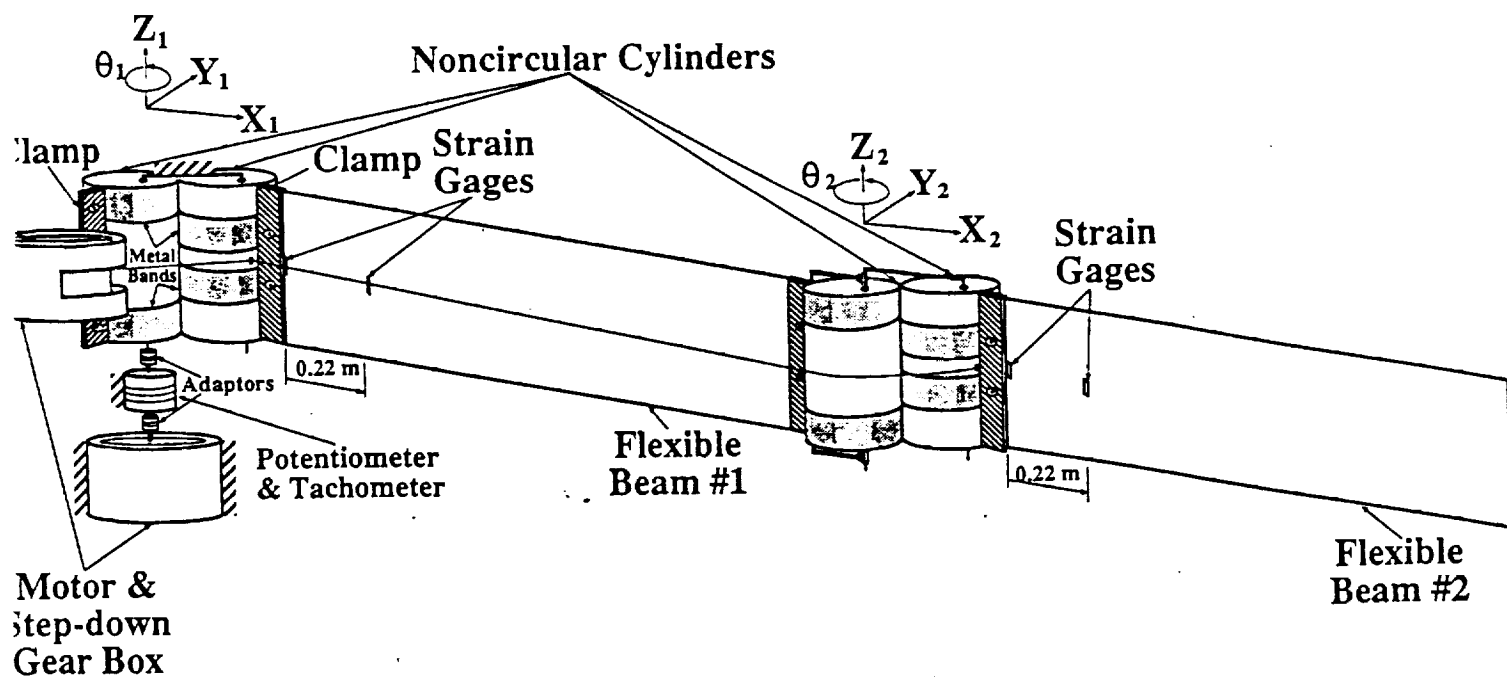


Figure 5: Configuration of two planar flexible beams

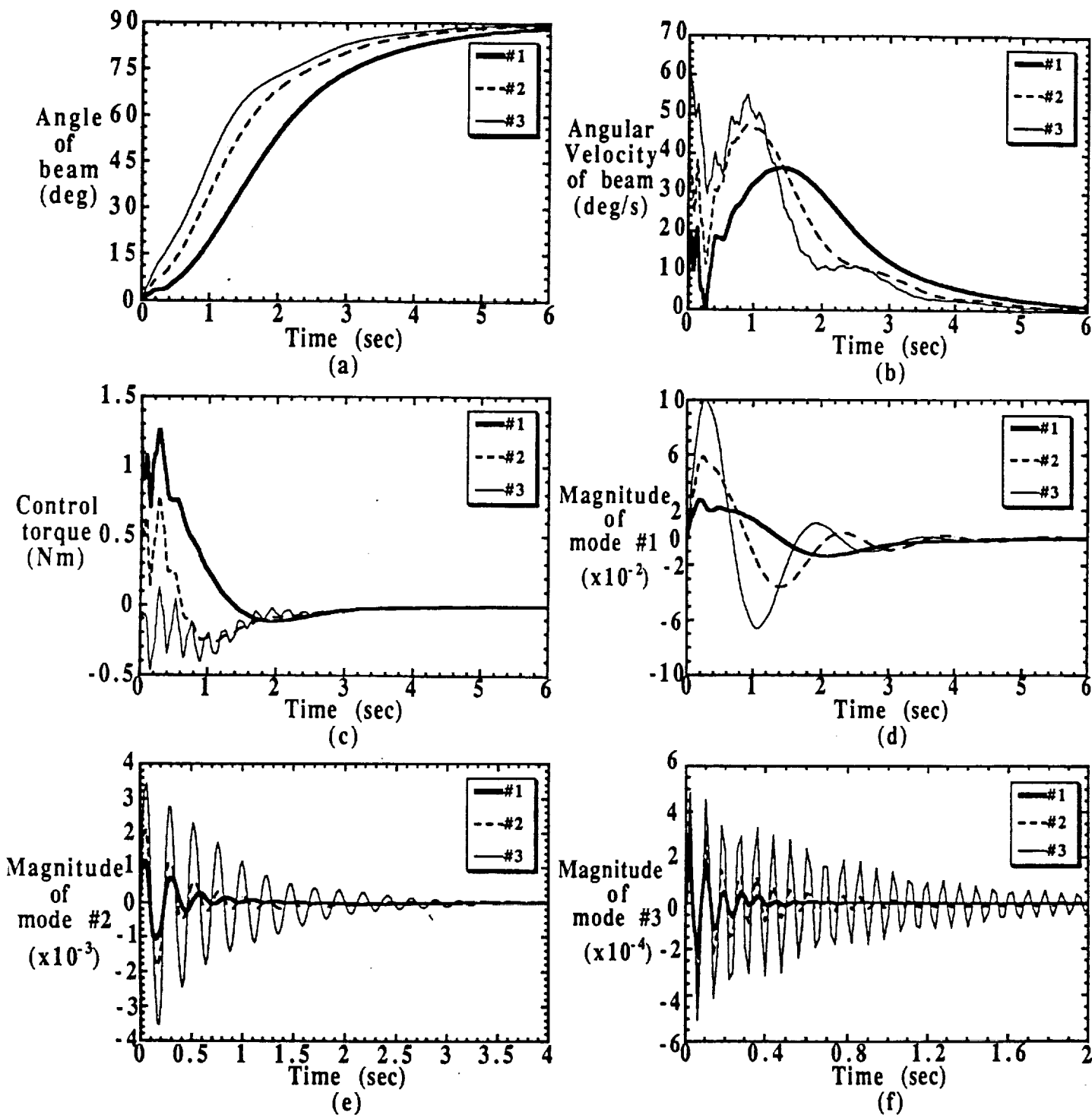


Figure 6: Simulation results of a planar flexible beam for a 90° slew maneuver

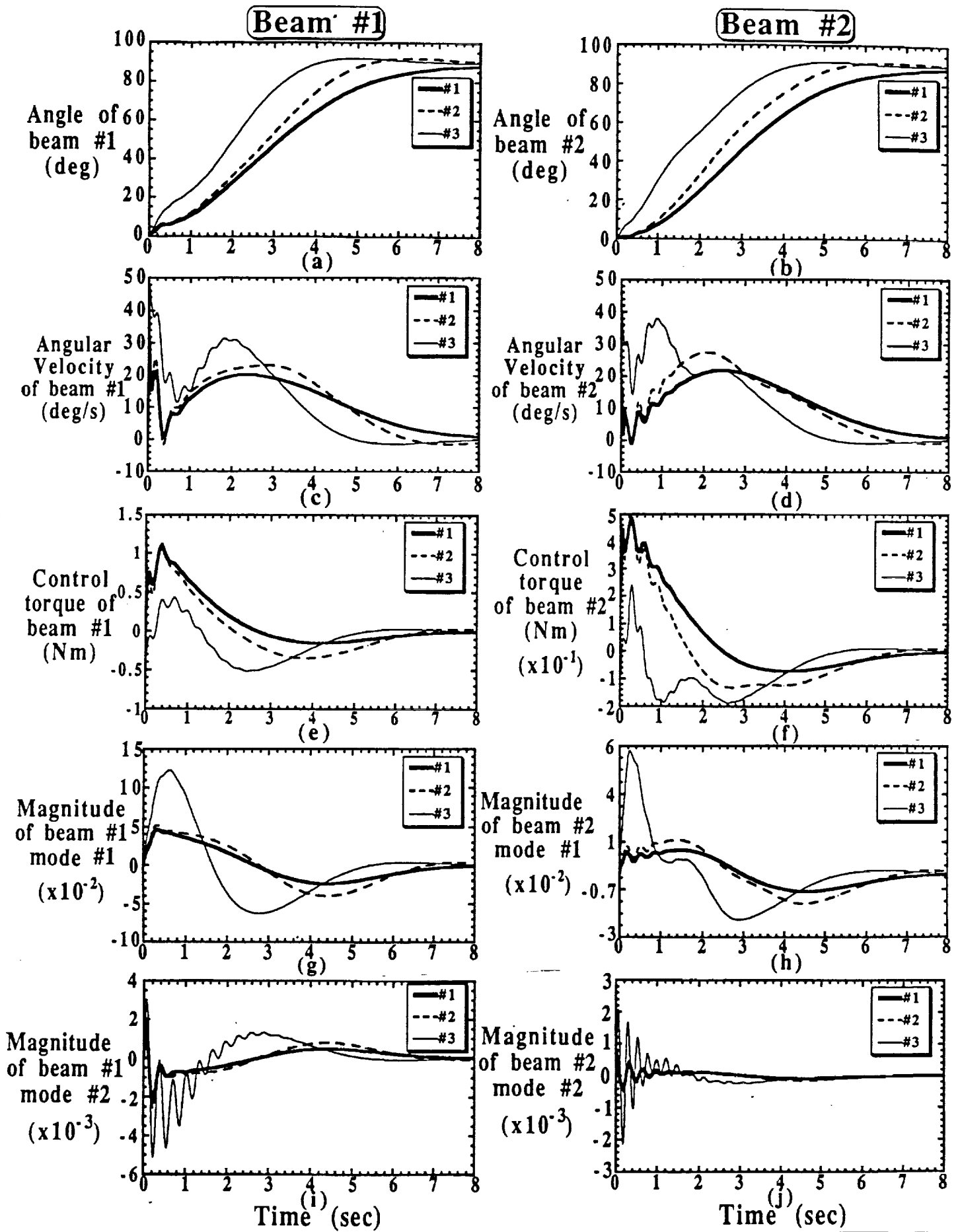


Figure 7: Simulation results of two planar flexible beams for a 90° slew maneuver